Available online at www.sciencedirect.com
ScienceDirect
Ceramics International 40 (2014) 3755–3759
CERAMICS INTERNATIONAL
www.elsevier.com/locate/ceramint

Enhanced piezoelectric coefficient of HfO_2-modified $(K_{0.44}Na_{0.56})_{0.94}Li_{0.06}(Nb_{0.94}Sb_{0.06})O_3$ lead-free ceramics

Tao Chen[a,*], Hongli Wang[b], Ting Zhang[a], Guangchang Wang[a], Jifang Zhou[a], Jianwei Zhang[a], Yuhong Liu[a]

[a]*Teaching and Research Section of Physics, Chengdu Medical College, Chengdu 610083, PR China*
[b]*Teaching and Research Section of Chemistry, Chengdu Medical College, Chengdu 610083, PR China*

Received 3 September 2013; received in revised form 9 September 2013; accepted 11 September 2013
Available online 20 September 2013

Abstract

$(K_{0.44}Na_{0.56})_{0.94}Li_{0.06}(Nb_{0.94}Sb_{0.06})O_3$–$x$$HfO_2$ (KNLNS–$x$$HfO_2$) lead-free piezoceramics were prepared using the conventional solid-state method, and effects of HfO_2 content on their microstructure and electrical properties were investigated. Their phase structure is independent of the HfO_2 content (x=0–0.008). As the HfO_2 content increases, the grain size, the Curie temperature, and the dielectric constant decrease. The ceramic with x=0.004 has enhanced electrical properties, i.e., d_{33}~266 pC/N, k_p~42.1%, ε_r~950, tanδ~0.027, and T_C~343 °C, showing that adding HfO_2 enhances the piezoelectric properties of KNLNS ceramics.

Keywords: C. Piezoelectric properties; Lead-free ceramics; (K,Na)NbO_3; HfO_2

1. Introduction

$Pb(Zr,Ti)O_3$ (PZT)-based piezoceramics have been widely used in some electronic devices because of their excellent piezoelectric properties and high Curie temperature (T_C) [1]. However, the PZT ceramics give rise to environmental pollution during their preparation and processing due to the volatilization of lead element which is a toxic substance [1,2]. Much attention has been paid on the ABO_3-type lead-free piezoelectric materials in order to protect the environment [3–20], such as $BaTiO_3$, $Bi_{0.5}Na_{0.5}TiO_3$, and $(K_{0.5}Na_{0.5})NbO_3$ (KNN). Among those, KNN-based lead-free piezoceramics have received considerable attention as a promising candidate for the PZT ceramics because of their excellent piezoelectric properties and high Curie temperature [2,9–22].

The pure KNN ceramic has a low piezoelectric constant (d_{33}) of ~80–100 pC/N and a high T_C of ~420 °C [2]. In addition, it is difficult to obtain the dense KNN ceramics because of the volatilization of the potassium element during their sintering process [2,23]. In the past several years, some preparation techniques have been used to produce the dense KNN ceramics, including hot pressing and spark plasma sintering [2,23]. The new preparation techniques which can improve the density and electrical properties of the KNN ceramics, have not been used widely yet in view of expensive elements and complicated preparation routes [2,23]. Recently, research results have shown that the sintering as well as electrical properties except d_{33} (<250 pC/N) of KNN ceramics can be improved by ABO_3-type addition, for example, $BaTiO_3$, $SrTiO_3$, $CaTiO_3$, $LiSbO_3$, $LiTaO_3$, $LiNbO_3$, and $SrTiO_3$, but their d_{33} is still poor (<250 pC/N) [2,10,11,13,14,16]. It was reported that the addition of HfO_2 can enhance the piezoelectric properties of one piezoelectric material [22–25]. For example, Zhou et al. reported that (Ba,Ca)(Ti,Hf)O_3 ceramics have a giant d_{33} of ~550 pC/N [24]. Moreover, a large d_{33} of ~446–680 pC/N is also observed in $Pb(Hf_{0.445}Ti_{0.555})O_3$–$Pb(Mg_{1/3}Nb_{2/3})O_3$ and $Bi(Ni_{1/2}Hf_{1/2})O_3$–$PbTiO_3$ ceramics [25,26]. However, there were few reports with regard to the effect of HfO_2 content on the electrical properties of the KNN-based ceramics.

In this work, $(K_{0.44}Na_{0.56})_{0.94}Li_{0.06}(Nb_{0.94}Sb_{0.06})O_3$–$x$$HfO_2$ (KNLNS–$x$$HfO_2$) lead-free piezoceramics were prepared using the conventional solid-state method, and effects of HfO_2

*Corresponding author.
E-mail addresses: chentaocmc@163.com, myfriendsroom@163.com (T. Chen).

0272-8842/$ - see front matter
http://dx.doi.org/10.1016/j.ceramint.2013.09.045

content on their microstructure and electrical properties were studied. Enhanced d_{33} is achieved in KNLNS–$x$$HfO_2$ by tuning the HfO_2 content, and the related physical mechanism was also addressed.

2. Experimental procedure

$(K_{0.44}Na_{0.56})_{0.94}Li_{0.06}(Nb_{0.94}Sb_{0.06})O_3$–$x$$HfO_2$ (x=0, 0.002, 0.004, 0.006, and 0.008) lead-free piezoelectric ceramics were prepared using the conventional mixed oxide sintering method. In this work, raw materials were K_2CO_3 (99%), Na_2CO_3 (99.8%), Li_2CO_3 (99%), Nb_2O_5 (99.5%), Sb_2O_3 (99%), and HfO_2 (99.999%). These powders were weighed and ball milled by the zirconia ball using ethanol for 24 h, and then dried and calcined at 800 °C for 5 h. The calcined powders were mixed with 8 wt% polyvinyl alcohol (PVA) solution, and then pressed into pellets with a diameter of 10 mm and a thickness of 1.2 mm under single direction pressure of about 15 MPa. The green pellets were sintered at 1080–1095 °C for 2 h. Silver electrodes were pasted on both surfaces of the sintered samples by firing at 600 °C for 10 min, and then these samples were polarized at 30 °C in the silicon oil using an electric field of 3–4 kV/mm for 30 min.

X-ray diffraction (XRD, D8-2-Advanced, BRUKER AXS, German) was used to determine the phase structure of the sintered ceramics. Dielectric properties vs. temperatures were characterized using an LCR meter (HP4284A, Hewlett-Packard, USA) equipped with a programmable temperature box. Surface morphologies of the sintered samples were measured using the scanning electron microscopy (SEM, JSM-5610LV, JEOL, Japan). The density was measured using the Archimedes method with distilled water. The piezoelectric constant (d_{33}) was measured using a quasistatic piezoelectric d_{33} meter (ZJ-3A, Institute of Acoustics, Chinese Academy of Sciences, China) after 24 h aging, and the planar coupling coefficient (k_p) and the mechanical quality factor (Q_m) were determined using the resonance–anti-resonance technique and an impedance analyzer (Agilent 4294A). P–E hysteresis loops of the ceramics were measured at 10 Hz using a radiant precision workstation (USA).

3. Results and discussion

The XRD patterns of KNLNS–$x$$HfO_2$ ceramics are measured at room temperature, as shown in Fig. 1(a). All the ceramics have a pure perovskite structure and there are no secondary phases, indicating the formation of stable solid solutions between KNLNS and HfO_2. That is, there is only single-phase perovskite structure without secondary phases. To characterize the evolution of the phase structure, the expanded XRD patterns are indicated in Fig. 1(b). A tetragonal phase was observed in all the ceramics regardless of the HfO_2 content [17], as confirmed by the temperature-dependent dielectric constant [Fig. 3]. It was found that the diffraction peaks shift to a lower angle as the HfO_2 content increases because of partly substitution of the Hf^{4+} for the Nb^{5+}, the ionic radius of which is nearly 0.064 nm and smaller than that of Hf^{4+} (~0.079 nm) [27].

Surface micrographs of KNLNS–$x$$HfO_2$ ceramics with x=0, 0.04, and 0.08 were measured by the SEM, as shown in Fig. 2 (a)–(c). The grain size gradually decreases as the HfO_2 doping level increases. As a result, the addition of HfO_2 can adjust the microstructure and refine the grain size of KNLNS ceramics. The decrease of the grain size should be mainly assigned to different ionic radii of Nb^{5+} and Hf^{4+}. It was reported that the ion with a larger ionic radius and atomic weight can easily reduce the mobility of the ions, which leads to the decrease of the grain size [28,29].

To study the effect of the HfO_2 content on their phase transitions as a function of the temperature, the curves of the temperature-dependent dielectric properties are shown in Fig. 3 (a)–(c). One phase transition was observed in these ceramics, which corresponds to the tetragonal–cubic phase transition (T_C) [13]. T_C slowly decreases as the HfO_2 content gradually increases, showing that HfO_2 slightly affects T_C of KNLNS ceramics. A similar phenomenon was demonstrated in

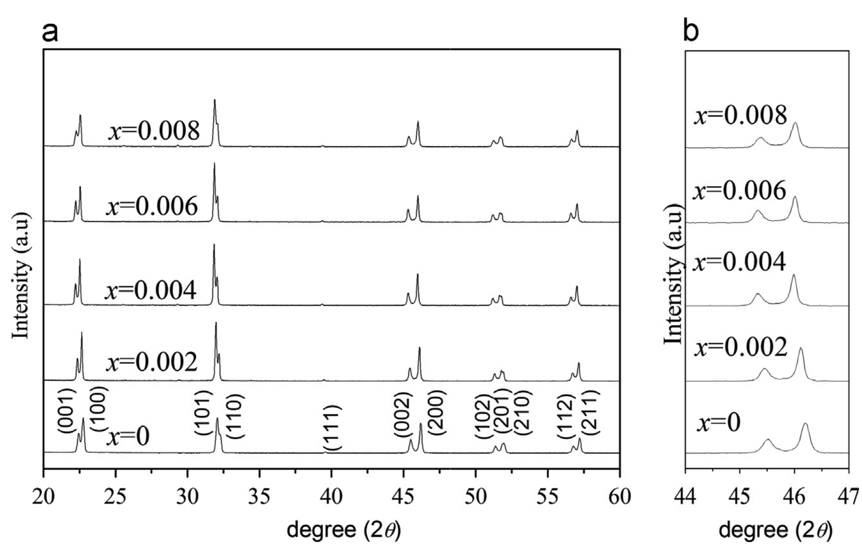

Fig. 1. XRD patterns of KNLNS–$x$$HfO_2$ ceramics: (a) 20–60° and (b) 44–47°.

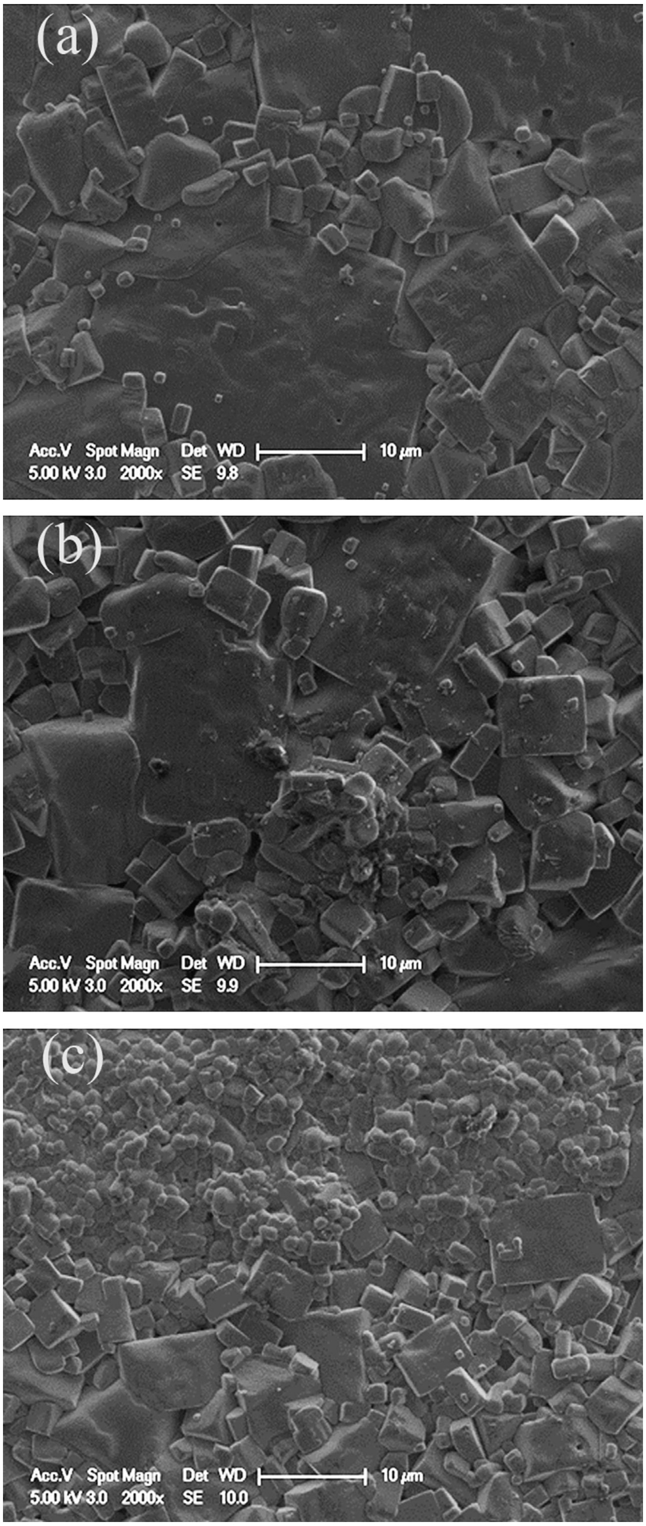

Fig. 2. SEM surface micrographs of KNLNS–xHfO$_2$ ceramics with (a) $x=0$, (b) $x=0.004$, and (c) $x=0.008$.

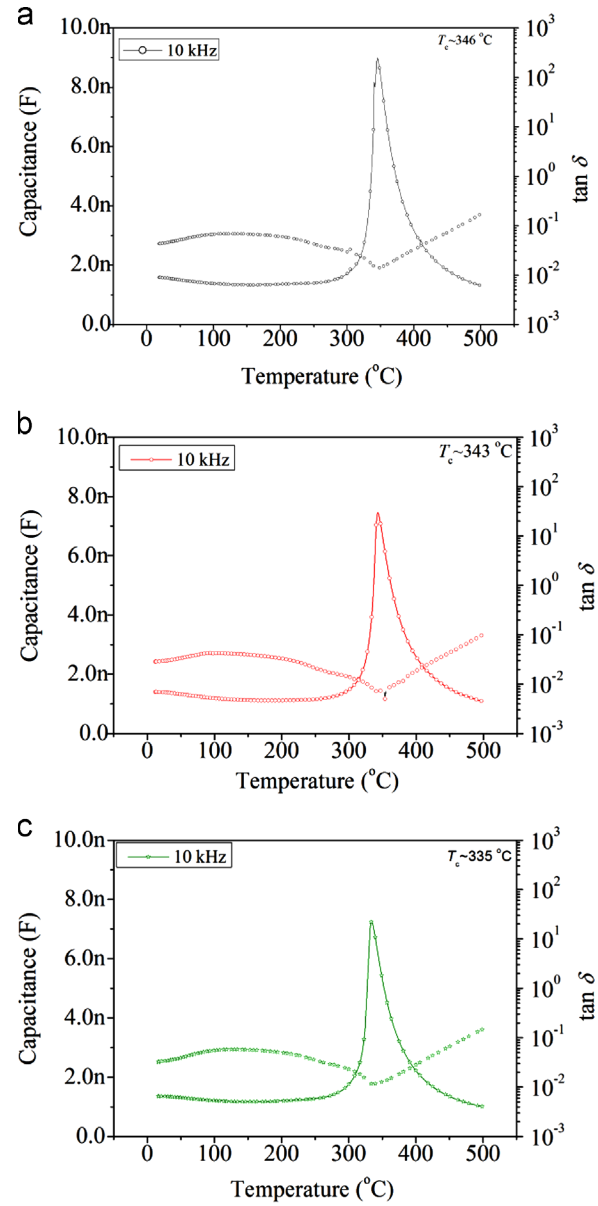

Fig. 3. Temperature-dependent dielectric properties in KNLNS–xHfO$_2$ ceramics with (a) $x=0$, (b) $x=0.004$, and (c) $x=0.008$.

HfO$_2$-modified piezoelectric materials [28]. In addition, the ceramic with $x=0.004$ has a lower dielectric loss (tanδ) because of a denser microstructure.

Fig. 4 shows the dielectric behavior of KNLNS–xHfO$_2$ ceramics as a function of HfO$_2$ content, measured at room temperature. It was found that tanδ and ε_r gradually decrease with an increase in the HfO$_2$ content[29], which reveals that ε_r and tanδ are sensitive to the HfO$_2$ content. It was reported that the grain size strongly affects the ε_r of functional materials [28]. Cai et al. reported that smaller grain size results in a lower ε_r because the ε_r of the grain is larger than that of the grain boundary [27]. As a result, the addition of HfO$_2$ leads to the enhanced dielectric behavior of KNLNS–xHfO$_2$ ceramics.

Fig. 5 plots the piezoelectric properties of KNLNS–xHfO$_2$ ceramics, measured at room temperature. d_{33} increases as the HfO$_2$ content increases, reaches a maximum value of ~266 pC/N at $x=0.004$, and decreases as the HfO$_2$ content further increases. Similar to the change of d_{33}, k_p also exhibits a similar trend, reaching a maximum value (i.e., ~42.1%). However, Q_m remains almost unchanged with the variation of the HfO$_2$ content ($x=0$–0.008). As a result, the enhanced piezoelectric behavior of

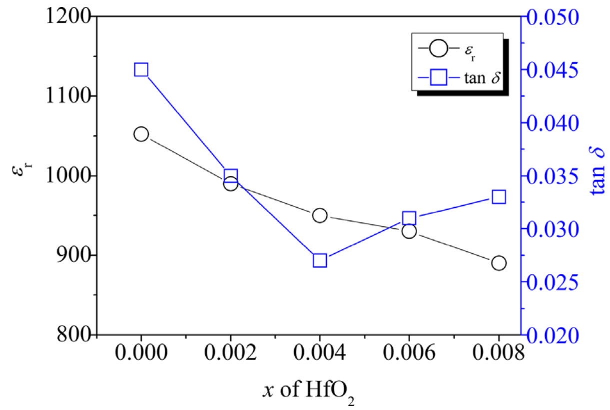

Fig. 4. Dielectric properties of KNLNS–xHfO$_2$ ceramics.

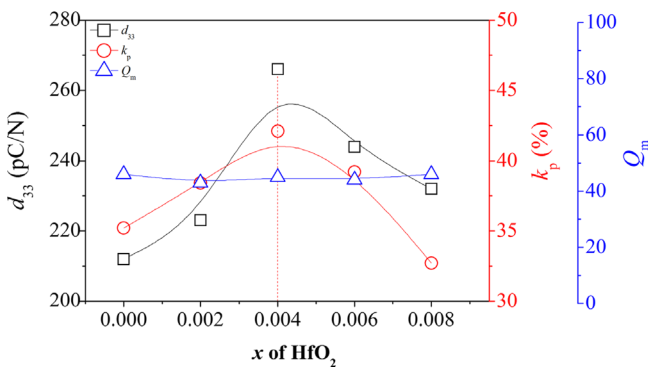

Fig. 5. Piezoelectric properties of KNLNS–xHfO$_2$ ceramics.

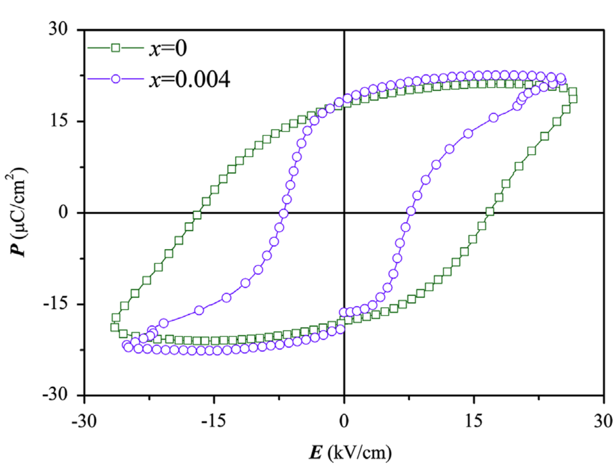

Fig. 6. Ferroelectric properties of KNLNS–xHfO$_2$ ceramics.

this work could be attributed to the addition of optimum HfO_2 content, together with a denser microstructure.

Fig. 6 shows the polarization–electric field (P–E) hysteresis loops of the ceramics with $x=0$ and 0.004, measured at 10 Hz and room temperature. All the ceramics show a typical saturated P–E loop, while an obvious difference is also observed. It was found that a "fat" P–E loop is shown in the ceramic with $x=0$, while the ceramic with $x=0.004$ has a slimmer and more saturated P–E loop. In addition, the ceramic with $x=0.004$ has a much smaller E_C value than that of the pure one, showing that the domain of the ceramic with $x=0.004$ is more easily rotated under a lower electric field. A similar result was observed in Hf -modified $BaTiO_3$ ceramics [27].

4. Conclusions

The conventional solid-state method was used to prepare the KNLNS–xHfO$_2$ lead-free piezoceramics, and their microstructure and piezoelectric properties are very sensitive to the HfO_2 content. All the ceramics have a tetragonal phase, which is independent of the small content of HfO_2 addition investigated in this study. The addition of HfO_2 results in a reduction in the grain size, while their T_C value remains almost unchanged. The ceramic with $x=0.004$ has an enhanced piezoelectric behavior (i.e., $d_{33}\sim266$ pC/N and $k_p\sim42.1\%$). As a result, the piezoelectric properties of KNN-based ceramics could be improved by adding HfO_2.

Acknowledgments

Authors gratefully acknowledge the supports of the Chengdu Medical College and the Scientific Research Foundation of the Education Department of Sichuan Province, China (09ZC085).

References

[1] B. Jaffe, W.R. Cook, H. Jaffe, in: Piezoelectric Ceramics, Academic, New York, 1971.

[2] J. Rödel, W. Jo, K.T.P. Seifert, E.M. Anton, T. Granzow, D. Damjanovic, Perspective on the development of lead-free piezoceramics, Journal of the American Ceramic Society 92 (2009) 1153–1177.

[3] W.F. Liu, X.B. Ren, Large piezoelectric effect in Pb-free ceramics, Physical Review Letters 103 (2009) 257602.

[4] J. Wu, D. Xiao, B. Wu, W. Wu, J. Zhu, Z. Yang, J. Wang, Sintering temperature-induced electrical properties of $(Ba_{0.90}Ca_{0.10})(Ti_{0.85}Zr_{0.15})O_3$ lead-free ceramics, Material Research Bulletin 47 (2012) 1281–1284.

[5] W. Li, Z. Xu, R. Chu, P. Fu, G. Zang, Piezoelectric and dielectric properties of $(Ba_{1-x}Ca_x)(Ti_{0.95}Zr_{0.05})O_3$ lead-free ceramics, Journal of the American Ceramic Society 93 (10) (2010) 2942–2944.

[6] J. Wu, D. Xiao, W. Wu, Q. Chen, J. Zhu, Z. Yang, J. Wang, Composition and poling condition-induced electrical behavior of $(Ba_{0.85}Ca_{0.15})(Ti_{1-x}Zr_x)O_3$ lead-free piezoelectric ceramics, Journal of the European Ceramic Society 32 (2012) 891–898.

[7] D. Lin, D. Xiao, J. Zhu, P. Yu, Piezoelectric and ferroelectric properties of $[Bi(NaKLi)]TiO_3$ lead-free piezoelectric ceramic, Applied Physics Letters 88 (2006) 062901.

[8] T. Chen, T. Zhang, G.C. Wang, J.F. Zhou, J.W. Zhang, Y.H. Liu, Effect of $Li_{0.12}Na_{0.88}NbO_3$ content on the electrical properties of $Bi_{0.50}Na_{0.50}$-TiO_3 lead-free piezoelectric ceramics, Journal of Alloys and Compounds 520 (2012) 7–10.

[9] S. Zhang, R. Xia, T.R. Shrout, Lead-free piezoelectric ceramics vs. PZT?, Journal of Electroceramics 19 (2007) 251–257.

[10] Y. Guo, K. Kakimoto, H. Ohsato, Phase transitional behavior and piezoelectric properties of $(Na_{0.5}K_{0.5})NbO_3$–$LiNbO_3$ ceramics, Applied Physics Letters 85 (2004) 4121–4123.

[11] R.Z. Zuo, D.Y. Lv, J. Fu, Y. Liu, L.T. Li, Phase transition and electrical properties of lead free $(Na_{0.5}K_{0.5})NbO_3$–$BiAlO_3$ ceramics, Journal of Alloys and Compounds 476 (2009) 836–839.

[12] Y. Zhao, R. Huang, R. Liu, X. Wang, H. Zhou, Enhanced dielectric and piezoelectric properties in Li/Sb-modified (Na, K)NbO_3 ceramics by optimizing sintering temperature, Ceramic International 39 (2013) 425–429.

[13] C. Wattanawikkam, N. Vittayakorn, T. Bongkarn, Low temperature fabrication of lead-free KNN–LS–BS ceramics via the combustion method, Ceramics International 39 (2013) S399–S403.

[14] F. Rubio-Marcos, J.J. Reinos, X. Vendrell, J.J. Romero, L. Mestres, P. Leret, J.F. Fernández, P. Marchet, Structure, microstructure and electrical properties of Cu^{2+} doped (K,Na,Li)(Nb,Ta,Sb)O_3 piezoelectric ceramics, Ceramics International 39 (2013) 4139–4149.

[15] J. Wu, D. Xiao, Y. Wang, J. Zhu, W. Shi, W. Wu, B. Zhang, J. Li, Phase structure, microstructure and ferroelectric properties of $(1-x)$ $[(K_{0.50}Na_{0.50})_{0.94}Li_{0.06}]$ $(Nb_{0.94}Sb_{0.06})O_3$–$x$$CaTiO_3$ lead-free ceramics, Journal of Alloys and Compounds 476 (2009) 782–786.

[16] H. Du, W. Zhou, F. Luo, D. Zhu, S. Qu, Y. Li, Z. Pei, Structure and electrical properties' investigation of $(K_{0.5}Na_{0.5})NbO_3$–$(Bi_{0.5}Na_{0.5})TiO_3$ lead-free piezoelectric ceramics, Journal of Physics D: Applied Physics 41 (2008) 085416.

[17] X. Cheng, J. Wu, X. Wang, B. Zhang, J. Zhu, D. Xiao, X. Wang, X. Lou, Giant d_{33} in (K,Na)(Nb,Sb)O_3–(Bi,Na,K, Li)ZrO_3 based lead-free piezoelectrics with high T_c, Applied Physics Letters 103 (2013) 052906.

[18] Y. Gao, J. Zhang, Y. Qing, Y. Tan, Z. Zhang, X. Hao, Remarkably strong piezoelectricity of lead-free $(K_{0.45}Na_{0.55})_{0.98}Li_{0.02}(Nb_{0.77}Ta_{0.18}Sb_{0.05})O_3$ ceramic, Journal of the American Ceramic Society 94 (9) (2011) 2968–2973.

[19] Z.P. Yang, Effects of composition on phase structure, microstructure and electrical properties of $(K_{0.5}Na_{0.5})NbO_3$–$LiSbO_3$ ceramics, Materials Science and Engineering A 432 (2006) 292–298.

[20] F. Rubio-Marcos, P. Marchet, J.J. Romero, J.F. Fernandez, Structural, microstructural and electrical properties evolution of (K,Na,Li)(Nb,Ta,Sb) O_3 lead-free piezoceramics through NiO doping, Journal of the European Ceramic Society 31 (2011) 2309–2317.

[21] F. Rubio-Marcos, J.J. Romero1, J.F. Fernández, P. Marchet, Control of the crystalline structure and piezoelectric properties of (K,Na,Li)(Nb,Ta, Sb)O_3 ceramics through transition metal oxide doping, Applied Physics Express 4 (2011) 101501.

[22] T. Chen, H. Wang, T. Zhang, G. Wang, J. Zhou, J. Zhang, Y. Liu, Piezoelectric behavior of $(1-x)K_{0.50}Na_{0.50}NbO_3$–$x Ba_{0.80}Ca_{0.20}ZrO_3$ lead-free ceramics, Ceramics International 39 (2013) 6619–6622.

[23] T.R. Shrout, S.J. Zhang, Lead-free piezoelectric ceramics: alternatives for PZT?, Journal of Electroceramics 19 (2007) 111–124

[24] C. Zhou, W. Liu, D. Xue, X. Ren, H. Bao, J. Gao, L. Zhang, Triple-point-type morphotropic phase boundary based large piezoelectric Pb-free material—$Ba(Ti_{0.8}Hf_{0.2})O_3$–$(Ba_{0.7}Ca_{0.3})TiO_3$, Applied Physics Letters 100 (2012) 222910.

[25] D. Wang, M. Cao, S. Zhang, Piezoelectric properties of $PbHfO_3$–$PbTiO_3$–$Pb(Mg_{1/3}Nb_{2/3})O_3$ ternary ceramics, Physica Status Solidi (RRL)—Rapid Research Letters 6 (2012) 135–137.

[26] Z. Pan, J. Chen, L. Fan, L. Liu, L. Fang, X. Xing, High piezoelectric performance in a new Bi-based perovskite of $(1-x)Bi(Ni_{1/2}Hf_{1/2})$ $O_3-xPbTiO_3$, Journal of Applied Physics 112 (2012) 114120.

[27] J. Chen, C. Fu, W. Cai, G. Chen, S. Ran, Microstructures, dielectric and ferroelectric properties of $BaHf_xTi_{1-x}O_3$ ceramics, Journal of Alloys and Compounds 544 (2012) 82–86.

[28] W. Cai, C. Fu, J. Gao, Z. Lin, X. Deng, Effect of hafnium on the microstructure, dielectric and ferroelectric properties of $Ba[Zr_{0.2}Ti_{0.8}]O_3$ ceramics, Ceramics International 38 (4) (2012) 3367–3375.

[29] S. Halder, T. Schneller, R. Waser, S.B. Majumder, Electrical and optical properties of chemical solution deposited barium hafnate titanate thin films, Thin Solid Films 516 (2008) 4970–4976.